Electrochemical deposition with a forced fluid flow inducing a transition from dendrites to disordered ramified morphologies

S. Fautrat[1] and P. Mills[1,2]
[1]*Laboratoire de Biorhéologie et d'Hydrodynamique Physico-chimique, URA 343 CNRS, Université Paris VII, 2 place Jussieu, 75251 Paris Cedex 05, France*
[2]*Laboratoire de Recherche sur les Matériaux dans leur Environnement, Université de Marne la Vallée, 2 rue du promontoire, 93166 Noisy le Grand Cedex, France*
(Received 31 July 1995)

Centripetal convection is imposed in a radial quasi-two-dimensional cell during the electrochemical deposition of zinc. At low flow rates the side branches of the dendrites are shortened. Beyond a flow rate threshold a transition is observed, leading to disordered ramified morphologies with fractal properties comparable to diffusion-limited aggregation. In this second regime, shadowgraphs show that the inhomogeneous region surrounding the deposit is narrower with a larger flow rate; in addition, the length scale of metal compactness is greatly increased (by several tens of micrometers). An interpretation in terms of migrative transport is proposed that would explain the morphological similarities with the patterns commonly produced by the association of Laplacian growth and unstable tips.

PACS number(s): 81.10.Aj, 81.15.Lm, 68.70.+w, 82.45.+z

I. INTRODUCTION

A. Theoretical stakes

Electrodeposits obtained from aqueous solutions of a metal salt, under nonequilibrium conditions, offer a rich variety of patterns. In a first approximation these patterns can be split into three classes [1–7]. First there exist dentritic crystal patterns, which show a straight main direction given by the growth of a stable tip, with side branches forming a fixed angle with this direction, where the value of the angle depends on the growth regime. The second class is that of disordered patterns, which do not show straight directions of growth, the tips undergoing repeated splittings. Some of these patterns have well-established fractal properties [5,6], and resemble the clusters produced by the diffusion-limited aggregation (DLA) computer simulation of Witten and Sander [8,9]. The third group consists of dense patterns that are also characterized by unstable tips, but with the remarkable differences that there are a stable overall outline and a homogeneous filling of space.

Though the various observed structures are all ramified, the ramification processes are different. During dendrite formation, the side branches grow in definite directions, each branching process corresponding to a well-defined crystal angle. In contrast, fractal deposits are not characterized by any particular crystal angle, although there is evidence for a certain probability distribution for each screening angle between branches of two successive generations [6]. This presence of widely varying situations has become a subject of active discussion. The role of microscopic anisotropy has been demonstrated [3,10] and the interplay of different involved fields has been noted [11], but the mechanism of morphology determination remains an open question. This subject also is of concern in other fields like crystallization [12,13], fluid fingering [14–17] erosion [18], and, also, biology [1,19], where similar patterns are obtained.

Electrodeposition of a metal with fast kinetics (i.e., not limiting the growth process) constitutes a paradigm for studying the role of additional contributions to diffusive transport, e.g., migration and convection, in the pattern formation.

B. Convection and the morphology selection problem

Several experiments have demonstrated the existence of local electrically driven convection near certain growing deposits [20,21]. This convection occurs in regions of the cell located near the deposit, where the space charge is not negligible. Convection due to gravity also has been reported [22,23]. It occurs in large portions of the cell as soon as the salt concentration is sufficient to allow a large density difference between the bulk and the depleted regions.

A few experiments with controlled convection in the context of the study of morphology selection of large electrodeposits have been published. Jorné, Lii, and Yee have found that a convection of the electrolyte, applied against the dendrite tips, reduces the roughness [24]. With a convection field making an angle with the electrical field, Laura-Tomàs *et al.* have observed that the growing direction is bent toward the convection direction [25,26]; at small length scales the roughness is reduced as in the experiment of Jorné *et al.* The bending also is observed in some computer simulations involving a ''convection effect'' making an angle with the diffusive transport [26–29].

In this paper we describe several experiments that differ from those quoted above. First, our field geometries are both radial, so the angle between the convection and electrical fields was kept small; second, we explored a larger range of convection speeds. At large length scales the deposits thus obtained reveal different morphologies.

C. Predictions by computer simulation

Meakin [30] introduced a simple convection effect through a bias in the DLA algorithm (anisotropy in the motion of the aggregating particule), and found a morphology

 © 1996 The American Physical Society

transition from DLA to dense patterns. Nagatani [31] extended this work to circular geometry. He obtained the same transition with centripetal convection, and a transition to one-dimensional patterns with centrifugal convection. He concluded that centripetal and centrifugal flows respectively increase and decrease the fractal dimension.

We are not aware of electrodepositions reported in the literature that can be compared with these results. Our experiments concern the radial geometry, but our initial morphology is a dendrite, not the DLA. Nevertheless, with a centripetal flow we obtained a transition leading to a denser pattern (larger fractal dimension), since the rectilinear dendrite is changed into a deposit of the DLA type.

D. Summary of the experimental results and their possible interpretation

Starting from experimental conditions leading to the dendrite morphology, we apply a centripetal flow of electrolyte (aqueous solution of zinc sulfate). At low flow rates there is a first regime where the dendritic shape is preserved, but with shorter side branches. At larger flow rates there is a second regime where the dendrite is replaced with a disordered deposit looking like the DLA clusters grown with an increased surface tension [9,32]. We wonder whether the geometrical characteristics of the second regime can be explained by the usual model for DLA growth, i.e., the model that assumes that a pure ''Laplacian'' transport (interface speed controlled by a Laplace equation), associated with fluctuations destabilizing the growing tips, leads to fractal aggregates [1,8,9,33].

II. EXPERIMENT

A. Device and observation without forced convection

All the experiments reported in this paper were conducted in circular geometry with $1M$ zinc sulfate aqueous solution. The experimental device is drawn in Fig. 1. A Plexiglas disk (15-mm radius) and a glass plate form a sandwich containing a solution layer of thickness $e=145$ μm, constrained by three peripheral spacers. The anode is a zinc wire ring surrounding the disk. The central cathode is a properly cut medical needle of 400-μm external diameter. A plastic tube, together with an inner electric wire, are set at the upper end of this needle. A voltage of 3.50 V is applied between the two electrodes. Direct views are obtained from a charge-coupled device (CCD) camera, as well as shadowgraphs, when a light source giving a parallel beam (lens with point source at focal point) and a diffusing screen are inserted.

The experimental conditions (cell geometry, voltage, initial concentration) were chosen to provide dendritic morphologies, like the one presented in Fig. 2(a), not too far off from the conditions for the disordered aggregates in the morphology diagram [2,3]. During such electrochemical deposition the concentration field has a complex structure [22,34,35]: the quasihomogeneous bulk is separated from the deposit by a zone of large gradient showing up on interferograms or shadowgraphs [Fig. 2(b)].

The basic idea is to reduce large scale inhomogeneity by means of a radial flow of the solution. This is achieved by withdrawing the cell solution through the needle. We used a

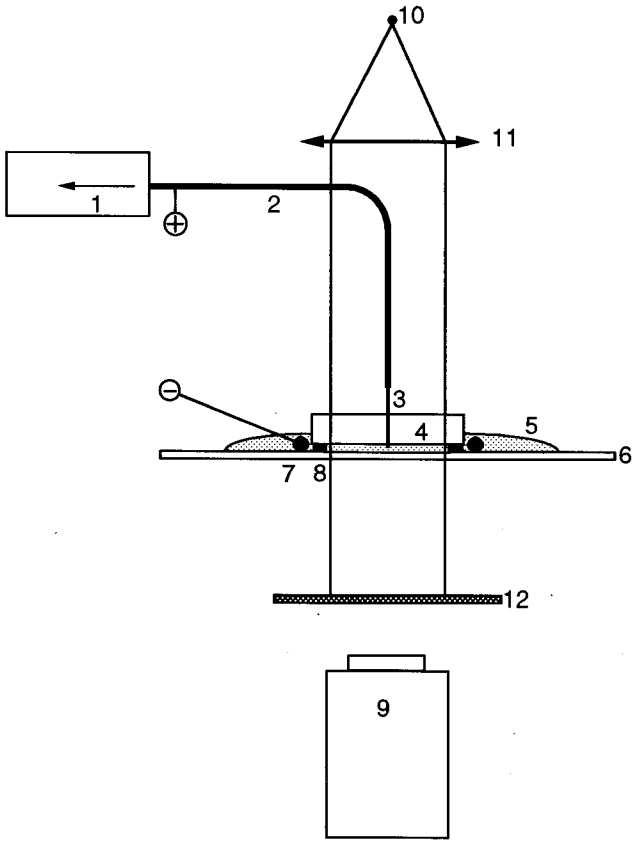

FIG. 1. Cell, pumping, and image systems: (1) pump; (2) tube allowing the creation of a radial flow inside the cell (the tube contains an inner wire connected to the generator); (3) medical needle (ϕ=0.4 mm) serving as cathode; (4) Plexiglas disk (ϕ=30 mm); (5) $ZnSO_4$ solution whose level is kept steady during the pumping process; (6) glass plate; (7) Zn anode surrounding the disk; (8) spacers (thickness $e=145$ μm); (9) CCD camera. Additional device for shadowgraphs: (10) point source; (11) lens; (12) diffusing screen. The parallel light rays going through the solution layer reveal, when refracted, the inhomogeneous regions.

Harvard pump (type 44), with regular syringes, in order to control the flow rate value (Q); then the speed (v) averaged over the thickness (e), at a given radius (r), can be calculated from $v=Q/2\pi re$.

B. Results with centripetal convection

At every run the pump was activated several minutes prior to the polarization of the cell.

The deposit shape is changed in a manner depending on the chosen flow rate. At low values (0.1 ml/h, for example) the dendrite shape is still present but the difference in growth rate between the main and the side directions is amplified. Figure 3(a) shows an example. The persistency of a large and well defined inhomogeneous zone encompassing the deposit is confirmed by the shape of the bright line in the shadowgraph of Fig. 3(b). At higher values of Q, above 0.5 ml/h, the deposits no longer present a stable growth direction and look like the disordered patterns. Figures 4(a) and 5(a) show two examples for, respectively, 2 and 5 ml/h. With such forced convections, the inhomogeneous zone loses its regular structure and is confined in the vicinity of the deposit [Figs. 4(b)

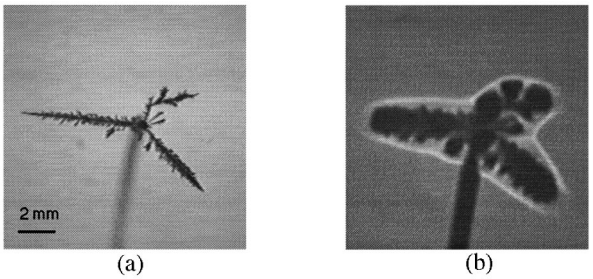

FIG. 2. (a) Dendritic electrodeposit grown from aqueous solution of zinc sulfate, without forced fluid flow. Concentration 1 mol/l. Voltage 3.50 V. The cell is described in Fig. 1. The upper tube of Fig. 1 gives an image in the lower part of Fig. 2(a), but of no importance for image digitizing. (b) Shadowgraph of the same deposit taken during the growth process. The parallel light rays (see Fig. 1) are bent when going through solution regions presenting a concentration gradient. Thus, one can distinguish two kinds of regions: (i) the quasihomogeneous bulk, (ii) bright lines encompassing the deposit area, indicating gradient zones (the solution being depleted in the inner region).

and 5(b)]. The branches become thicker [compare the micrographs of Figs. 6(a) and 6(b)], in such a way that the deposits ressemble DLA clusters grown with large capillary length [9,32]. When the branches become thick enough the deposits are robust and can be recovered undamaged.

The crossover in the growth dynamics can be quantitatively exhibited through a study of the growth rate and of the deposited mass. During each electrodeposition, when the radius was changing from 1 to 7 mm, the electric current intensity and the time were recorded, in order to compute the average speed of the fastest tip as well as the deposited mass. The plot of velocities as a function of the flow rate (Fig. 7) clearly displays two regimes, with a crossover value of about 0.5 ml/h. The plot of masses (Fig. 7) presents a step at the same value, but less spectacularly.

From digitized images, a common box counting [1] has been performed to determine a fractal dimension. The deposits exhibiting a good linear fitting (of fractal nature) have dimensions contained between 1.64 and 1.76 (Fig. 8). These values are close to 1.71, the fractal dimension of DLA clusters [36].

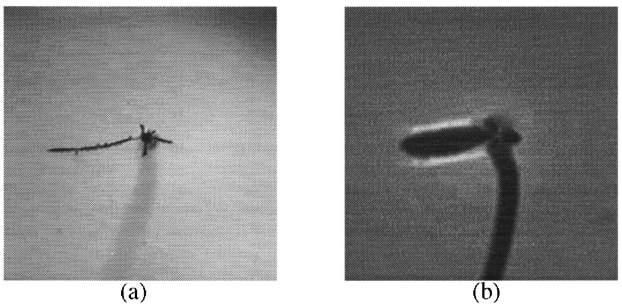

FIG. 3. (a) Dendritic electrodeposit grown under the same conditions as in Fig. 2, but with a centripetal forced fluid flow; the flow rate is 0.1 ml/h. The side branches are shorter than in Fig. 2. Same magnification as in Fig. 2. (b) Shadowgraph of the same deposit taken during the growth process. The bright lines still indicate a well defined and large inhomogeneous zone reflecting the dendrite symmetry.

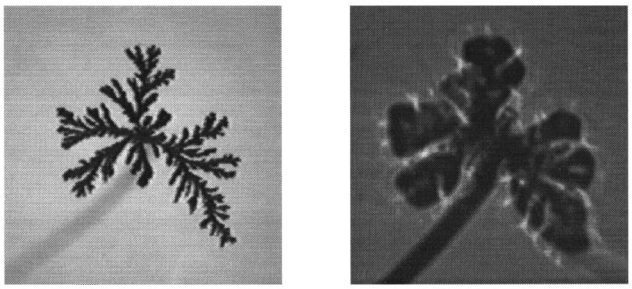

FIG. 4. (a) Electrodeposit grown under the same conditions as in Fig. 2, but with a centripetal forced fluid flow; the flow rate is 2 ml/h. The shape is very different from that in Fig. 2 and resembles DLA clusters grown with diffusing particles. Same magnification as in Fig. 2. (b) Shadowgraph of the same deposit taken during the growth process. The bright lines lack the regular structure observed in Figs. 2(b) and 3(b), and they progressively disappear when the flow rate is increased.

III. THEORETICAL DISCUSSION

A. Tip destabilization

Numerous works [1,17,37–41] have shown that the tip stability is controlled by the competition between the microscopic anisotropy (which furnishes preferential growth directions) and fluctuations of various origins (which favor changes of direction). During the growth of dendrites the crystal anisotropy is sufficient to maintain a stable tip only if the curvature radius is small, of the order of micrometers [42–44], as in Fig. 6(a). Otherwise, two surface elements with appreciable orientation difference (surface energy difference) are too distant to sustain an anisotropy effect. With sufficient forced convection the large curvature radius [tens of micrometers, Fig. 6(b)] moves the system away from this condition and the tip stability becomes unlikely. Furthermore, additional fluctuations associated with the forced flow (disturbance of the flow due to the growing deposit, etc.), must be a function of the flow rate and particularly active at high values.

B. Geometrical properties

For a ramified deposit one can evaluate a characteristic length, which plays the role of a capillary length. Below this scale compact domains are found, and above this scale ramified structures are noted. For well developed deposits obtained in the second regime, this length is at least of several tens of micrometers [Fig. 6(b), for example]. At larger scales of observation the extension of inhomogeneous regions in the electrolyte is less significant. The building of the ramified structure can be shown to be mainly controlled by the electrical field. Indeed, each flux of the charged species is [45]

$$\mathbf{j}_i = -c_i u_i z_i F \nabla \phi - D_i \nabla c_i + c_i \mathbf{v},$$

where the index i stands either for cations or anions, c is the local concentration, z the charge number of one ion, F the Faraday constant, u the mobility, ϕ the electric potential, D the diffusivity, and $\mathbf{v}$ the convection speed vector. The electric current density is

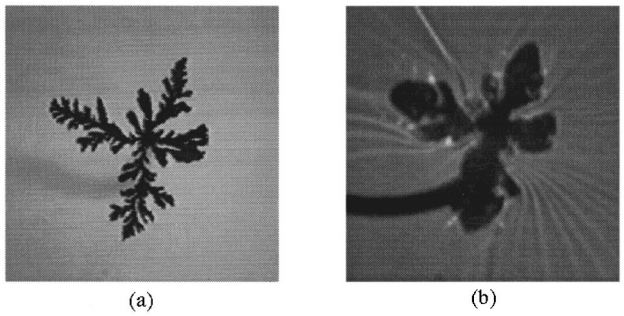

FIG. 5. (a) Electrodeposit grown under the same conditions as in Fig. 2, but with a centripetal forced fluid flow; the flow rate is 5 ml/h. (b) Shadowgraph of the same deposit taken during the growth process. The inhomogeneous (dark) zones are confined in the deposit vicinity. Some bright lines coming from the outer perimeter indicate current lines of more concentrated solution; they must correspond to instabilities in the electrodissolution process at the peripheral anode.

$$\mathbf{j}=\sum (z_i F \mathbf{j}_i)$$

$$=-\sum (c_i u_i z_i^2 F^2)\nabla\phi-\sum (z_i F D_i)\nabla c_i+\sum (z_i F c_i)\mathbf{v}.$$

At the length scales of interest, the last two terms vanish since both the concentration gradients and the space charge $\Sigma(z_i F c_i)$ are negligible. Thus the convection does not explicitly appear, and the current is Ohmic. Moreover the conservation of the deposing element gives a relation between the cations flux $j_{c\perp}$, normal to the interface, and the interface speed $v_\perp$:

$$j_{c\perp}=(c_{\text{solid}}-c_{\text{surf}})v_\perp \approx (c_{\text{solid}})v_\perp ,$$

where c_{solid} (concentration inside the cathode)$\gg c_{\text{surf}}$ (cation concentration next to the interface). The normal electric current $j_\perp$ through the interface is due to the sole reacting species, so

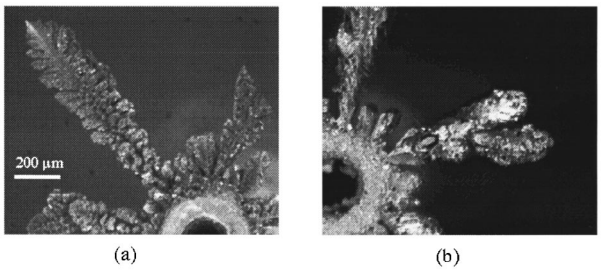

FIG. 6. (a) Micrograph of electrodeposit grown under the same conditions as in Fig. 2 (no forced flow). Observations at larger magnifications show tips with short curvature radius (of the order of a micrometer). The deposit still presents a ramified structure at that length scale. (b) Micrograph of electrodeposit grown under the same conditions as in Fig. 5 (flow rate 5 ml/h). The deposit is smooth at short length scales and ramified at large length scales, the crossover value now being larger than the 10 μm (and even larger for larger growth durations). The tips are rounded and do not present correlation with crystal axis. Same magnification as in Fig. 6(a).

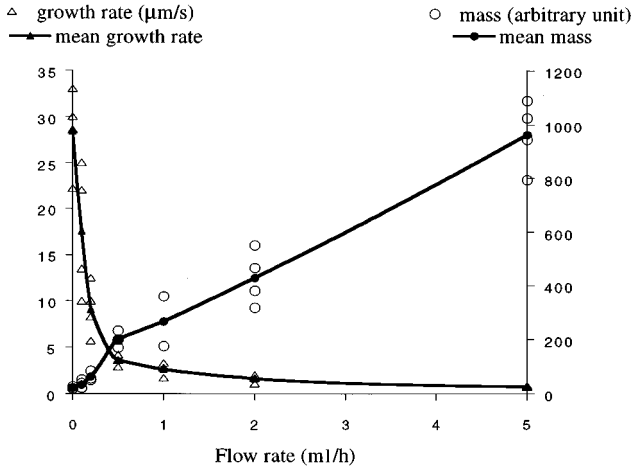

FIG. 7. Growth rates and deposited masses for different flow rates imposed inside the cell. Each growth rate is the velocity of the fastest tip averaged over its motion from 1- to 7-mm radius. Each mass is calculated from the electric current during the same period. For each flow rate, the mean values for growth rate and mass were calculated. The smooth fitting of the velocity distribution exhibits two distinct parts: (i) rapidly decreasing between 0 and 0.5 ml/h, (ii) quasisteady low value (still with a slow decrease) beyond 0.5 ml/h. The mass curve exhibits a step at the same crossover value (around 0.5 ml/h). Some experimental data are superposed when plotted.

$$j_\perp = z_c F j_{c\perp};$$

hence the growth rate $v_\perp$ is also proportional to $j_\perp$, and so proportional to the normal electrical field $(-\nabla\phi)_\perp$. Also in the quasielectroneutrality approximation ϕ satisfies the Laplace equation. Finally, with the potential assumed constant at each electrode surface, the set of equations for the Laplacian growth [1] is obtained. If this interpretation is correct, one has a new experiment showing that DLA patterns are obtained, provided the tips are unstable and the interface speed directly depends on a Laplacian field [1,8,9,33].

IV. CONCLUSION

We have shown that for the radial cell geometry, with conditions of voltage and concentration ordinarily giving

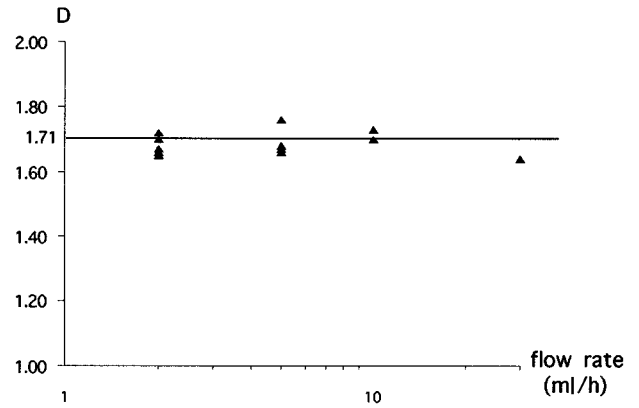

FIG. 8. Fractal dimensions of deposits grown with centripetal forced flow. The method is the box counting applied to the digitized images of the deposits. Some runs presenting moderate linear fitting have been excluded. The obtained values should be compared with the dimension of DLA clusters (1.71).

dendrites, one can obtain deposits resembling the DLA clusters if one imposes a sufficient centripetal convection of the electrolyte. Furthermore the transition to DLA clusters appears only after exceeding a threshold in the flow rate values. In these conditions, a large part of the electrolyte is found to be quasihomogeneous, with the exception in the vicinity of the growing interface. The length scale of metal compactness is found much larger than in the usual electrodeposition experiments performed in quasi-two-dimensional cells.

We have also shown that, besides the tip instability, at length scales larger than the compactness scale, the transport may be considered as close to pure migration, and so the growth equations are formally similar to those of DLA

Concerning the existence of two different regimes we wonder if it can be studied through some stability analysis performed in the electrodeposition context [46–49]; for example, Chen and Jorné [46] have obtained two regimes for the evolution of the amplification factor when an increasing convection is taken into account.

The computer simulations of Nagatani [31] exhibit larger fractal dimensions when there is a centripetal convection effect. Although the present experiments are qualitatively consistent with this result, we think that the usual algorithms are not relevant to electrodeposition. Indeed, in this case the transport is described by the current density, which, because of the electroneutrality condition, does not contain convection terms. The convection acts through the concentration parameter (c), which is present in its diffusive and migrative terms (besides the current density expression, c is determined by the whole set of equations relevant to a cell subjected to convection). Furthermore the difficult problem of transition between stable and unstable tips should be included in some way.

The present work only focused on a special case, and studies of other growth conditions including controlled convections could contribute to more general understanding of convection effects.

[1] T. Vicsek, *Fractal Growth Phenomena* (World Scientific, Singapore, 1992).

[2] Y. Sawada, A. Dougherty, and J. P. Gollub, Phys. Rev. Lett. **56**, 1260 (1986).

[3] D. Grier, E. Ben-Jacob, R. Clarke, and L. M. Sander, Phys. Rev. Lett. **56**, 1264 (1986).

[4] D. Grier, D. A. Kessler, and L. M. Sander, Phys. Rev. Lett. **59**, 2315 (1987).

[5] M. Matsushita, M. Sano, H. Hayakawa, H. Honjo, and Y. Sawada, Phys. Rev. Lett. **53**, 286 (1984).

[6] F. Argoul, A. Arneodo, J. Elezgaray, G. Grasseau, and R. Murenzi, Phys. Rev. A **41**, 5537 (1990).

[7] P. D. Trigueros, J. Claret, F. Mas, and F. Sagueès, J. Electroanal. Chem. **312**, 219 (1991).

[8] T. A. Witten and L. M. Sander, Phys. Rev. Lett. **47**, 1400 (1981).

[9] T. A. Witten and L. M. Sander, Phys. Rev. B **27**, 5686 (1983).

[10] E. Ben-Jacob and P. Garik, Physica D **38**, 16 (1989).

[11] P. Garik, D. Barkey, E. Ben-Jacob, E. Bochner, N. Broxholm, B. Miller, B. Orr, and R. Zamir, Phys. Rev. Lett. **62**, 2703 (1989).

[12] J. S. Langer, Rev. Mod. Phys. **52**, 1 (1980).

[13] H. Honjo, S. Ohta, and M. Matsushita, Phys. Rev. A **36**, 4555 (1987).

[14] L. Paterson, J. Fluid. Mech. **113**, 513 (1981).

[15] S. N. Rausseo, P. D. Barnes, and J. V. Maher, Phys. Rev. **35**, 1245 (1987).

[16] R. Lenormand, Physica A **140**, 114 (1986).

[17] E. Ben-Jacob and P. Garik, Physica D **38**, 16 (1989).

[18] P. Mills, P. Cerasi, and S. Fautrat, Europhys. Lett. **29**, 215 (1995).

[19] E. Ben-Jacob, O. Schochet, A. Tenenbaum, I. Cohen, A. Czirok, and T. Vicsek, Nature **368**, 46 (1994).

[20] V. Fleury, J.-N. Chazalviel, and M. Rosso, Phys. Rev. Lett. **68**, 2492 (1992).

[21] V. Fleury, J.-N. Chazalviel, and M. Rosso, Phys. Rev. E **48**, 1279 (1993).

[22] D. P. Barkey, D. Watt, Z. Liu, and S. Raber, J. Electrochem. Soc. **141**, 1206 (1994).

[23] M. Rosso, J.-N. Chazalviel, V. Fleury, and E. Chassaing, Electrochimica Acta **39**, 507 (1994).

[24] J. Jorné, Y.-J. Lii, and K. E. Yee, J. Electrochem. Soc. **134**, 1399 (1987).

[25] L. Laura-Tomàs, J. Claret, and F. Sagués, Phys. Rev. Lett. **71**, 4373 (1993).

[26] L. Lopez-Tomàs, J. Claret, F. Mas, and F. Sagués, Phys. Rev. B **46**, 11 495 (1992).

[27] R. D. Poechy, A. Garcia, R. D. Freimuth, V. M. Castillo, and L. Lam, Physica D **51**, 539 (1991).

[28] A. P. Roberts and M. A. Knackstedt, Phys. Rev. E **47**, 2724 (1993).

[29] T. Nagatani and F. Sagués, Phys. Rev. A **43**, 2970 (1991).

[30] P. Meakin, Phys. Rev. B **28**, 5221 (1983).

[31] T. Nagatani, Phys. Rev. A **39**, 438 (1989).

[32] R.-F. Xiao, J. I. D. Alexander, and F. Rosenberger, Phys. Rev. A **38**, 2447 (1988).

[33] L. Niemeyer, L. Pietronero, and H. J. Wiesmann, Phys. Rev. Lett. **52**, 1033 (1984).

[34] P. Garik, J. Hetrick, B. Orr, D. Barkey, and E. Ben-Jacob, Phys. Rev. Lett. **66**, 1606 (1991).

[35] D. Barkey, J. Electrochem. Soc. **138**, 2912 (1991).

[36] S. Tolman and P. Meakin, Phys. Rev. A **40**, 428 (1989).

[37] E. Ben-Jacob, R. Godbey, N. D. Goldenfeld, J. Koplik, H. Levine, T. Mueller, and L. M. Sander, Phys. Rev. Lett. **55**, 1315 (1985).

[38] Y. Couder, O. Cardoso, D. Dupuy, T. Tarvernier, and W. Thom, Europhys. Lett. **2**, 437 (1986).

[39] E. Ben-Jacob and P. Garik, Nature **343**, 523 (1990).

[40] J. Kertész and T. Vicsek, J. Phys. A **19**, L257 (1986); J. Nittmann, and H. E. Stanley, Nature **321**, 663 (1986).

[41] M. Wang, N. Ming, and P. Bennema, Phys. Rev. E **48**, 3825 (1993).

[42] H. Honjo, S. Ohta, and Y. Sawada, Phys. Rev. Lett. **55**, 841 (1985).

[43] A. Dougherty, P. D. Kaplan, and J. P. Gollub, Phys. Rev. Lett. **58**, 1652 (1987).
[44] Y. Sawada, Physica A **140**, 134 (1986).
[45] J. S. Newman, *Electrochemical Systems* (Prentice Hall, Englewood Cliffs, NJ, 1973).
[46] C.-P. Chen and J. Jorné, J. Electrochem. Soc. **138**, 3305 (1991).
[47] D. P. Barkey, R. H. Muller, and C. W. Tobias, J. Electrochem. Soc. **136**, 2207 (1989).
[48] T. C. Halsey, Phys. Rev. A **36**, 3512 (1987).
[49] J. W. Diggle, A. R. Despic, and J. O'M. Bockris, J. Electrochem. Soc. **116**, 1503 (1969).